Bradley O. Elmore · John A. Bollinger
David M. Dooley

Human kidney diamine oxidase: heterologous expression, purification, and characterization

Abstract Human kidney diamine oxidase has been overexpressed as a secreted enzyme under the control of a metallothionein promoter in *Drosophila* S2 cell culture. This represents the first heterologous overexpression and purification of a catalytically active, recombinant mammalian copper-containing amine oxidase. A rapid and highly efficient purification protocol using chromatography on heparin affinity, hydroxyapatite, and gel filtration media allows for the recovery of large quantities of the recombinant enzyme, which is judged to be greater than 98% homogenous by SDS/PAGE. The availability of large quantities of highly purified enzyme makes it now possible to investigate the spectroscopic, mechanistic, functional, and structural properties of this human enzyme at the molecular level. Visible absorption, circular dichroism, electron paramagnetic resonance, and resonance Raman spectroscopic results are presented. The recombinant enzyme contains the cofactors 2,4,5-trihydroxyphenylalaninequinone and copper at stoichiometries of up to 1.1 and 1.5 mol per mol homodimer, respectively. In addition, tightly bound and stoichiometric calcium ions were identified and proposed to occupy a second metal-binding site. The apparent molecular weight of the recombinant protein, determined by analytical ultracentrifugation, suggests 20–26% glycosylation by weight. Detailed kinetic studies indicate the preferred substrates (k_{cat}/K_M) of human diamine oxidase are, in order, histamine, 1-methylhistamine, and putrescine, with K_M values of 2.8, 3.4, and 20 μM, respectively. These results, demonstrating the substrate preference for histamine and 1-methylhistamine, were unanticipated given the available literature. The pH dependence of k_{cat} for putrescine oxidation gives two a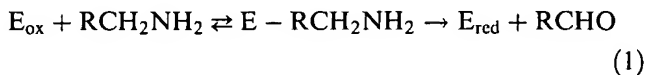pparent pK_a values at 6.0 and 8.2. Tissue-specific expression of the human diamine oxidase gene was investigated using an mRNA array. The relevance of this work to earlier work and the suggested physiological roles of the human enzyme are discussed.

Abbreviations *ABTS*: 2,2′-azinobis(3-ethylbenzthiazolinesulfonic acid · *CAO*: copper amine oxidase · *CHES*: 2-(*N*-cyclohexylamino)ethanesulfonic acid · *DAB*: *p*-dimethylaminomethylbenzylamine · *DAO*: diamine oxidase · *HEPES*: *N*-(2-hydroxyethyl)piperazine-*N*-(2-ethanesulfonic acid) · *hKDAO*: human kidney diamine oxidase · *MES*: 2-(*N*-morpholino) ethanesulfonic acid · *rhKDAO*: recombinant human kidney diamine oxidase · *TPQ*: 2,4,5-trihydroxyphenylalaninequinone

B.O. Elmore · J.A. Bollinger · D.M. Dooley (✉)
Department of Chemistry and Biochemistry,
Montana State University, Bozeman, MT 59717, USA
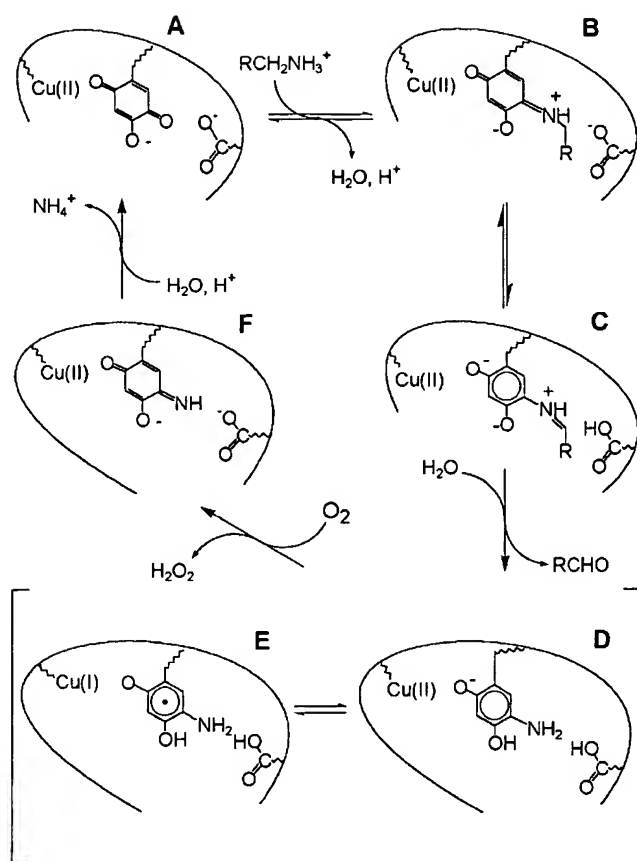E-mail: dmdooley@montana.edu
Fax: +1-406-9947989

Introduction

Copper-containing amine oxidases (E.C.1.4.3.6) catalyze the two-electron oxidative deamination of primary amines to the corresponding aldehyde, using dioxygen as the oxidant, with the concomitant production of ammonia and hydrogen peroxide. Catalysis proceeds through a ping-pong mechanism divided into two half-reactions (Eqs. 1, 2, and Scheme 1):

$$E_{ox} + RCH_2NH_2 \rightleftarrows E - RCH_2NH_2 \rightarrow E_{red} + RCHO \tag{1}$$

$$E_{red} + O_2 \rightarrow E_{ox} + H_2O_2 + NH_3 \tag{2}$$

Copper-containing amine oxidases (CAOs) are widespread in Nature, having been found in bacteria, yeasts and fungi, plants and animals. These enzymes are homodimers, generally ranging in size from 140 to 200 kDa, with two active sites per dimer [1]. Each active

Scheme 1. Proposed reaction mechanism for the oxidation of amines by copper-containing amine oxidases. The oxidized, resting enzyme (A) combines with amine substrate to give a substrate Schiff base (B). Proton abstraction by the conserved active-site aspartate from the substrate's α-carbon results in a product Schiff base and reduced TPQ (C). Product aldehyde is release by hydrolysis, leaving the aminoquinol form of the enzyme (D). This Cu(II)-aminoquinol is in equilibrium with a Cu(I)-aminosemiqui-none radical form (E). The enzyme is then oxidized, with dioxygen serving as the electron acceptor. Oxidation proceeds through a postulated aminoquinone intermediate (F), liberates ammonium and regenerates the resting enzyme (A)

site contains two cofactors: (1) a single type II copper ion, and (2) a quinone (2,4,5-trihydroxyphenylalanine-quinone, TPQ) derived from the post-translational modification of an invariant tyrosine residue [2]. TPQ has been shown to be produced in a novel, self-processing reaction requiring only copper and dioxygen [3, 4, 5, 6].

Three general classes of CAOs have been described from mammalian sources; unfortunately, the nomenclature in the literature is frequently confusing. One type of amine oxidase is found tightly associated with tissues, is active against monoamine substrates, and is commonly designated semicarbazide-sensitive amine oxidase (SSAO). It must be noted that all CAOs are inhibited by semicarbazide, so the designation of the tissue-associated amine oxidases as SSAOs is simply a convention. Sequence analysis has recently revealed these tissue-bound enzymes possess a single putative N-terminal

transmembrane helix [7]. Another variety of CAO is soluble, found in blood plasma, and is active against a wide range of monoamines, diamines, and aromatic amines. These enzymes are generally termed plasma amine oxidases, serum amine oxidases, or benzylamine oxidases, and are likely synthesized in the liver [8]. The third type of mammalian CAO is also soluble, but displays distinct substrate specificity for diamines. This group is therefore termed diamine oxidases (DAOs). These are also distinct in sequence homology from the soluble plasma and the membrane-bound CAOs [9, 10, 11].

Barbry and co-workers [12] identified the first complete sequence for a mammalian copper-containing diamine oxidase, that of the human kidney (previously misidentified as a protein associated with the amilo-ride-sensitive Na^+ channel). The translated cDNA sequence encodes a 751 amino acid polypeptide with a predicted 19 amino acid signal sequence for the classical secretory pathway. N-terminal sequencing of human DAO purified from kidney and placenta demonstrated the mature protein lacked these residues, confirming the predicted signal cleavage site. The amino acid sequence contains the copper amine oxidase consensus sequence T/SXXNYD/EY/N (residues 457–463), in which the first tyrosine residue is modified to TPQ in the mature enzyme. A heparin-binding consensus sequence, RFKRRLPK, was also recognized (residues 569–576).

The structures of four copper amine oxidases have been solved by X-ray crystallography: two are bacterial (*Escherichia coli* and *Arthrobacter globiformis*), one is from the yeast *Hansenula polymorpha* (formally classified as *Pichia angusta*), and one is from pea seedling (*Pisum sativum*) [13, 14, 15, 16]. Collectively these four enzymes exhibit considerable structural homology, although primary sequence identity is less than 40% between any two. The enzymes are "mushroom" shaped with an extensive intersubunit contact, including a pair of "arms" extending from each subunit to embrace the other. Three or four domains are in each monomer, including an N-terminal domain that forms the mushroom "stalk" (not present in all CAOs) and a large, C-terminal β sandwich catalytic domain.

The crystallographically determined structures confirm the copper coordination environment as predicted from spectroscopy [17, 18, 19]. The active-site copper ion is coordinated in a distorted square pyramidal geometry by three conserved histidine residues and two water molecules, one axial and the other equatorial. Also, the quinone cofactor is in close proximity to the copper ion and is observed in different conformations, indicative of inherent side-chain flexibility.

One unanticipated finding in the crystal structures of the *E. coli* and pea seedling CAOs was the identification of an additional metal-binding site in each subunit, modeled as being occupied by a calcium and a manganese ion, respectively. Three aspartate carboxylates, two peptide carbonyl oxygens, and one water molecule coordinate this second metal ion. These aspartate ligands

are absolutely conserved in all 10 sequenced mammalian CAOs, as well as in 16 of 25 sequences representing bacteria, fungi, plants, and animals. Seven additional organisms retain two of the three aspartates. The second-metal site and the inferred location of the heparin binding sequence are both on the solvent-exposed upper surface of the "mushroom cap" [14].

To date, direct examination of the mammalian diamine oxidase has been very limited, especially for the human enzyme. We report herein the heterologous overexpression and purification of recombinant human kidney DAO, the first successful overexpression of any mammalian copper-containing amine oxidase. Furthermore, high expression levels and a purification protocol described herein provide rapid and efficient recovery of significant quantities of the highly purified enzyme, as required for detailed investigations of its molecular properties. Initial characterization of the recombinant enzyme includes molecular weight determination, cofactor quantification, and measurement of its visible absorption, circular dichroism, electron paramagnetic resonance, and resonance Raman spectra. Steady-state kinetic parameters, pH dependence, and substrate specificity for the recombinant enzyme are reported. A tissue-specific expression profile for the human enzyme is presented, as is an analysis of the biological relevance of the enzyme.

Materials and methods

Expression cell line

The coding sequence for mature human kidney diamine oxidase was amplified by PCR from a cDNA clone (kindly provided by Dr. Barbry, Institut de Pharmacologie Moléculaire et Cellulaire, France) using Vent DNA Polymerase and appropriate primer adapters. The forward primer (5'-GTGAGATCTCCGGG-GACTCTGCCC) replaced the N-terminal codons for glutamic acid and proline of mature kidney DAO with the codon for arginine and introduced a *Bgl*II site. The reverse primer (5'-CCGGAATTCACGATGCCGGCCCTGGGCTGGGCC) introduced an *Eco*RI site just downstream from the native stop codon. The PCR product and the expression vector pMT/BiP/V5-His A (Invitrogen) were digested with *Bgl*II and *Eco*RI, agarose gel purified, recovered using Prep-A-Gene (Bio-Rad), and ligated with T4 DNA ligase. The 5' end of the resulting construct was confirmed by DNA sequencing (Silver Sequence, Promega) through the fusion site to an internal *Bst*II site, 350 base pairs into the coding sequence. The remainder of the coding sequence was swapped with a *Bst*II and *Eco*RI fragment from the cDNA clone to generate the expression vector pMTDAO. All DNA manipulations used enzymes from New England Biolabs. Constructs were maintained in *E. coli* strain TOP10 and purified using either Perfect Prep (5Prime3Prime) or Quantum Prep (Bio-Rad).

Transfection and cell culturing procedures were those outlined in the *Drosophila* Expression System Manual (Invitrogen), except as noted. Plasmids pMTDAO and the selection vector pCoHY-GRO were cotransfected into *Drosophila* Schneider 2 (S2) cells at a ratio of 19:1 (μg) using the Calcium Phosphate Transfection Kit (Invitrogen). Selection for the stably transfected subpopulation used 500 μg mL^{-1} hygromycin B (Roche Molecular Biochemicals). The resulting polyclonal cell line was adapted to and maintained in a serum-free medium (Ex-Cell 400, JRH Biosciences) supplemented with 300 μg mL^{-1} hygromycin B at 27 °C.

Expression and purification

The transfected cell line was expanded from a 5 mL culture in a 25 cm^2 tissue culture flask to a single 130 mL culture in a 250 mL spinner flask. When the spinner culture reached a density of 1×10^7 cells mL^{-1}, 25 mL of the culture was added to each of four 500 mL baffled shake flasks (Bellco Glass) containing 150 mL serum-free medium. The flasks were incubated in a gyrotary water bath at 110 rpm and 27 °C for about 24 h. At a density of 5×10^6 cells mL^{-1}, expression was induced by addition of copper sulfate to a final concentration of 500 μM, and incubation was then continued for 48 h. Nontransfected *Drosophila* S2 cells and the uninduced expression cell line were used as negative expression controls.

Cultures were harvested and cells spun out by centrifugation for 2 min at 1000×g. The supernatant was spun for 10 min at 10,000×g to remove particulates and then loaded on a 5 mL HiTrap Heparin HP column (Amersham Pharmacia Biotech) using a peristaltic pump. The column was then washed with 100 mM potassium phosphate buffer, pH 7.2, until A_{280} of the flow through reached zero, and bound protein was eluted with 100 mM potassium phosphate with 1 M sodium chloride, pH 7.2. The eluant was extensively dialyzed against 100 mM potassium phosphate, pH 7.2, and then loaded on Macro-Prep Ceramic Hydroxyapatite (type I, 40 μm particle size, Bio-Rad) in a HR 10/10 column using a FPLC system (Amersham Pharmacia Biotech). Buffers for the ceramic hydroxyapatite column were 100 mM potassium phosphate, pH 7.2 (buffer A) and 400 mM potassium phosphate, pH 7.2 (buffer B). Protein fractions were eluted with a two-column volume wash at 25% buffer B, a single column volume wash at 35% buffer B, and a two-column volume linear gradient from 35% to 100% buffer B. The most active fractions were pooled and concentrated in a 50 mL centrifugal concentrator (Millipore) before being run over a 1.6×100 cm Ultrogel AcA 34 (BioSepra) gel filtration column equilibrated in 100 mM potassium phosphate, pH 7.2. SDS/PAGE and IEF gels were by a PhastSystem (Pharmacia). Substantial absorbance at 280 nm in the culture media necessitated that initial protein concentration be determination by the Bradford protein assay (Bio-Rad) with bovine serum albumin standards. Subsequent protein concentrations were determined spectrophotometrically by absorbance at 280 nm using the predicted extinction coefficient for the mature, recombinant enzyme of 280.5 mM^{-1} cm^{-1} [20]. The extinction coefficient at 280 nm was later determined by magnetic circular dichroism and calculated as 297.6 mM^{-1} cm^{-1} (data not shown) [21].

Amine oxidase activity was measured at 37 °C in a stirred, thermostatted cuvette using a coupled assay with putrescine (dihydrochloride, Sigma) as the substrate. Assays used 30 U horseradish peroxidase (Sigma), 10 mM putrescine, and 2 mM ABTS [2,2'-azinobis(3-ethylbenzothiazoline-6-sulfonic acid)] in 100 mM potassium phosphate, pH 7.2, in a final volume of 2 mL. Reaction progress was followed spectrophotometrically by monitoring the change in absorbance at 414 nm ($\epsilon = 24.6$ mM^{-1} cm^{-1}) [22]. Activities measured by dioxygen depletion using an Instech oxygen electrode and chamber were in close agreement to those measured by the coupled assay (data not shown).

General characterization

UV and visible absorption data were acquired with either a Hewlett-Packard 8452A or 8453 diode-array spectrophotometer. CD spectra were obtained with a Jasco J-710 spectropolarimeter. Titrations with phenylhydrazine (HCl, Sigma) were used to quantify TPQ in the purified recombinant enzyme [23]. One mL of 10–20 μM protein in 100 mM potassium phosphate buffer was titrated with 2 μL aliquots of fresh, anaerobically prepared phenylhdrazine (~775 μM) at room temperature. Spectral changes were monitored and recorded after the absorbance at 445 nm reached a constant value following each addition (10–45 min). The derivatized enzyme was subsequently concentrated in a Microcon 30 (Millipore) with buffer exchange to remove unreacted phenylhydrazine. The concentrated phenylhydrazine-derivatized enzyme was then used for

resonance Raman spectroscopy on a Spex Triplemate spectrometer with a CCD detector, with excitation by a Coherent argon-ion laser. EPR spectra were recorded on a Bruker 220D SRC interfaced with a personal computer. Simulation of EPR spectra used the DOS EPR spectra manipulation program EPPER from Professor John Lipscomb (University of Minnesota), which incorporates the simulation program EPRGHA [24]. Copper, zinc, calcium, and magnesium analyses were performed by ICP emission spectroscopy (Little Bear Laboratories, Golden, Co.), or copper analysis by flame atomic absorption spectroscopy using a Buck Scientific model 210 VGP. Metal-free buffer was prepared by passage over Chelex-100 (Bio-Rad) and by using plasticware treated with 0.1 M EDTA solution. Analytical ultracentrifugation and ES/MS services were kindly provided by Andy Baron and Alison Ashcroft, respectively, at the University of Leeds, Leeds, UK.

Steady-state kinetics

K_M and k_{cat} were determined spectrophotometrically in a 37 °C thermostatted cell holder with magnetic stirring. Ionic strength of the assay buffer, 50 mM HEPES, pH 7.2, was maintained at 150 mM by addition of potassium chloride. Oxidation of p-dimethylaminomethylbenzylamine (DAB) and benzylamine were followed by the change in absorbance at 250 nm, using an extinction coefficient of 11 mM^{-1} cm^{-1} for p-dimethylaminomethylbenzaldehyde [25]. Assays with DAB or benzylamine used 890 μL of assay buffer and 10 μL enzyme in a 1 cm pathlength cuvette. This mixture was allowed to equilibrate for 2–3 min in the thermostatted cell holder before rapid addition of 100 μL substrate stock solution. Data acquisition was initiated immediately. All other assays used the coupled assay of Holt et al. [26] and an extinction coefficient for the quinoneimine dye of 6.00 mM^{-1} cm^{-1} at 498 nm [27]. Chromogen stock solution was prepared to give final concentrations of 1 mM 4-aminoantipyrine and 2 mM vanillic acid. Coupled assays used 880 μL chromogen stock solution, 10 μL (14.5 U) horseradish peroxidase, and 10 μL enzyme. Substrate, horseradish peroxidase, and chromogen stock solutions were freshly prepared in the assay buffer, and kept in a 37 °C water bath until use. Recombinant DAO was kept on ice. Thermal equilibration, substrate addition, and data acquisition were as described above. Assays used 10 μL of 4.37 μM recombinant human kidney DAO, or 4.09 μM enzyme in the case of 1-methylhistamine. Water bath and thermostatted cell holder temperatures were monitored with an electronic thermocouple. Initial rates were determined by at least duplicate experiments (most often triplicate) at six or more substrate concentrations and fitting to the Michaelis-Menten equation using Origin software (OriginLab). Those substrates demonstrating substrate inhibition were also fit to Eq. 3 [28]:

$$v = V_{max}[S]/\left(K_M + [S] + [S]^2/K_i\right) \qquad (3)$$

Substrates that oxidized either extremely slowly or at rates undetectable under these conditions were assayed up to millimolar substrate concentrations. Potential substrates were purchased commercially (highest grade available) and used without further purification, except for DAB, which was synthesized by the method of Bardsley et al. [25].

The pH dependence of Michaelis-Menten parameters for the oxidation of putrescine was determined using the coupled 4-aminoantipyrine/vanillic acid assay as described above. Buffers used were 50 mM MES (pH 5.69–6.33), 50 mM HEPES (pH 6.33–7.78), and 50 mM CHES (pH 8.12 and 8.85). Ionic strength was adjusted to a final concentration of 150 mM with potassium chloride. After equilibration at 37 °C, the pH was measured with an Orion perpHect LogR meter, model 310, equipped with an Automatic Temperature Compensation Probe. At least two (usually three or four) initial rates were determined at six or more substrate concentrations for each pH value. k_{cat} values were plotted against proton concentration and fit to the following equation [29]:

$$k_{cat} = (k_{cat})_{max}[H^+]pK_{a1}/\left(pK_{a1}pK_{a2} + pK_{a1}[H^+] + [H^+]^2\right) \qquad (4)$$

Enzyme stability in the pH range used was tested by incubation of the enzyme in the appropriate buffers for 15 min at 37 °C and then measuring the activity. Possible effects of pH on the quinoleimine dye generated during the assay were investigated by titrating hydrogen peroxide into the chromogenic solution plus horseradish peroxidase at appropriate pH values. Neither loss of enzyme activity nor change in quinoleimine dye absorption features was detected in the buffers and pH range investigated.

Heparin effects on enzyme activity were investigated by incubating recombinant kidney DAO with an approximately four-fold excess of heparin (from porcine intestinal mucosa, average molecular weight of 3000 Da, Sigma) over dimeric protein for 1 h on ice. Initial rate determinations for putrescine oxidation were as described above. The enzyme-heparin mix was stored at 4 °C and assayed for activity with 250 μM putrescine after 24, 48, and 72 h. All assays used air-saturated solutions and dissolved oxygen levels were not varied in these experiments (about 233 μM).

Tissue-specific gene expression

A Multiple Tissue Expression Array (Clontech) was used to determine the human, tissue-specific expression profile of human DAO. The manufacturer's instructions were followed for generating ^{35}P-labeled cDNA probes by random primer labeling, hybridization, and autoradiography.

Results

Expression and purification

The expression vector pMTDAO contains the coding sequence for mature human kidney diamine oxidase (hKDAO) fused to the *Drosophila* BiP signal sequence for secretion from *Drosophila* S2 cell culture. Expression is under the control of the *Drosophila* metallothionein promoter and induced by addition of copper sulfate to 500 μM. Mature recombinant human kidney diamine oxidase (rhKDAO) primary sequence, as deduced from the DNA sequence, differs from that of the natural protein in only the replacement of the N-terminal glutamic acid and proline with an arginine residue.

Culture media was harvested 48 h post-induction at a cell density of 1.45×10^7 cells mL^{-1}. Cells were greater than 99% viable, as determined by trypan blue staining, and exhibited normal morphology. No amine oxidase activity was detected in either the uninduced expression cell line or in the parental S2 cell line.

The recombinant enzyme is readily purified by heparin affinity chromatography, ceramic hydroxyapatite chromatography, and gel filtration; the summary of a typical purification is given in Table 1. Total enzymatic activity increases during the protocol and likely reflects the loss of an inhibiting substance (of either the amine oxidase or the coupled assay) that is present in the growth medium. The purified protein is estimated at greater than 98% homogeneous by SDS/PAGE, and the highest specific activity obtained from any purification was 1.25 IU mg^{-1}.

Table 1. Purification of recombinant human kidney diamine oxidase

Step	Total volume (mL)	Total protein (mg)	Total activity (IU)	Specific activity (IU mg^{-1})	Purification factor
Culture medium	630	117	7.3	0.063	1
Hi-Trap Heparin	13.5	41	12.5	0.30	4.8
Ceramic hydroxyapatite	44	14	13.0	0.93	14.8
Ultrogel AcA34	0.74	12	12.7	1.1	16.7
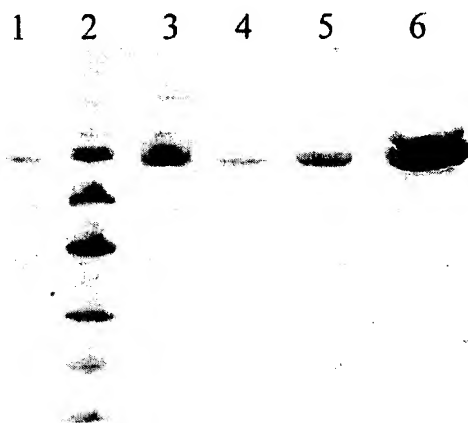
Fig. 1. SDS/PAGE showing purification of recombinant human kidney diamine oxidase. *Lane 1*: harvested *Drosophila* S2 media diluted 1:1 with gel loading buffer. *Lane 2*: molecular weight standards: 94, 67, 43, 30, 20.1, and 14.4 kDa. *Lane 3*: protein after Hi-Trap Heparin affinity column, 3.6 μg. *Lane 4*: following ceramic hydroxyapatite chromatography. *Lane 5*: purified protein after gel filtration chromatography, 2.4 μg. *Lane 6*: 9.6 μg of the rhKDAO. The distorted band is a consequence of the severe overloading of the gel; however, this lane demonstrates the high degree of purity for the recombinant enzyme

Purified rhKDAO is stable for several months when stored on ice. However, freezing the enzyme at −20 °C gives a significant drop in specific activity; thawed enzyme has about 40% the specific activity of that before freezing. Thawed protein can recover 85% of the original specific activity after storing on ice for 10 days. Bieganski and co-workers [30] have previously noted a 90% loss in activity with natural human DAO when stored at −20 °C.

Electrophoresis and analytical ultracentrifugation

Isoelectric focusing acrylamide gel electrophoresis gives an estimated pI of 6.2, and only a single protein band was observed. A pI of 6.7 is predicted from the primary sequence of rhKDAO [31]. Previous investigations reported isoelectric points of 6.0 and 7.1 for the natural human DAO [32, 33].

SDS/PAGE of the purified enzyme gives a single protein band with an apparent molecular weight of 94 kDa (Fig. 1), although the primary sequence of rhKDAO predicts 83.4 kDa for the mature monomer. No corresponding band is detected in negative controls. The ∼10 kDa discrepancy between the predicted and

observed molecular weights suggests the expressed protein is substantially glycosylated (vide infra). Literature values for the apparent molecular weight of the natural human DAO have been reported as 70, 90, and 105 kDa by SDS/PAGE [33, 34, 35]. As evident in Fig. 1, the recombinant protein band represents the major protein in harvested media.

Several attempts to determine the native molecular weight by acrylamide gel electrophoresis were unsuccessful. Gel filtration on a calibrated AcA 34 Ultrogel column gave an apparent molecular weight of 113 kDa, unrealistically low for the homodimer (data not shown). Interestingly, Crabbe et al. [34] reported native molecular weights for the purified human placental DAO as 70 kDa by Sephadex G-200 gel filtration and 69.5 kDa by polyacrylamide gel electrophoresis. However, sedimentation equilibrium ultracentrifugation data in the same work indicated a native molecular weight of 235 kDa. Baylin and Margolis [35] reported the native molecular weight of human pregnancy plasma DAO as close to 200 kDa, as determined with Sephadex G-200.

Sedimentation equilibrium ultracentrifugation of rhKDAO gave an average apparent molecular weight of 210 kDa (five runs with two protein concentrations at two speeds, data not shown). Curvature of the A_{280} versus radius plot suggests the recombinant enzyme is in reversible equilibrium between dimers and higher-order complexes. The data could equally fit dimer-tetramer, dimer-hexamer, or dimer-octamer models, with an association constant of 1.2 A_{280}^{-1} for the dimer-tetramer model.

Sedimentation velocity ultracentrifugation gave a sedimentation coefficient of 10 S and a diffusion coefficient of 4.4 Ficks (two runs, data not shown). The apparent molecular weight calculated by the Svedberg equation is 200 kDa. Both sedimentation velocity runs indicated a small shoulder of faster moving material, consistent with a very small amount of higher-order protein association.

Copper, calcium and TPQ

Copper, zinc, calcium, and magnesium content in the recombinant enzyme were investigated using either ICP emission spectroscopy or flame atomic absorption. Table 2 shows the results from three different enzyme preparations. The data suggest a mixture of copper and zinc occupying the active sites in the recombinant enzyme; the sum of copper and zinc approaches 2 mol per

Table 2. Metal ion and TPQ stoichiometry for rhKDAO as iso-lated from three enzyme purifications. Metal ion and TPQ values reported as mol per mol dimeric enzyme

Specific activity (IU mg^{-1})	Cu	Zn	Ca	Mg	TPQ
0.85	1.03	0.79	1.84	0.91	0.72
1.21	1.42[a]	ND[b]	ND	ND	1.04
1.25	1.48	0.40	3.20	0.0	1.08

[a]Value determined by flame atomic absorption spectroscopy; all other metal ion quantifications were by ICP emission spectroscopy
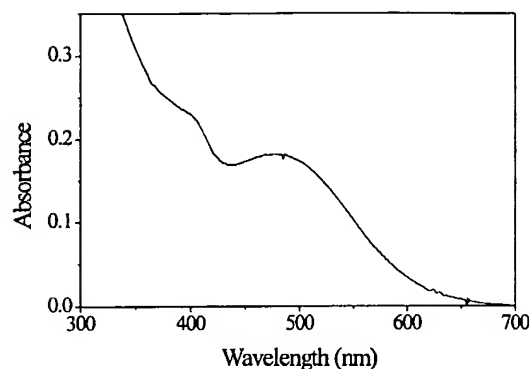[b]Not determined
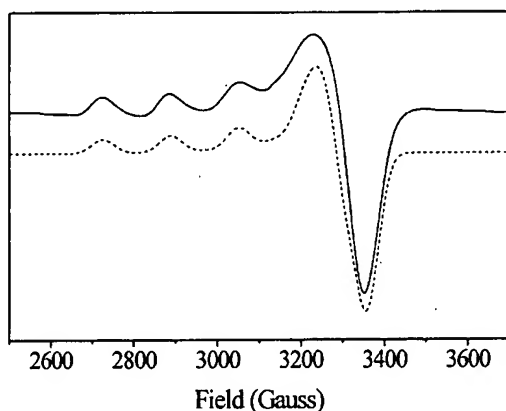
Fig. 2. X-band EPR spectra of the purified enzyme at ~200 μM in 100 M potassium phosphate buffer (*upper line*). The simulated spectra is shown with $g_\perp = 2.043$, $g_{||} = 2.265$, and $A_{||} = 162$ G (*lower dashed line*). Experimental conditions: 77 K, 9.42 GHz, 0.796 mW, 20 G modulation amplitude

Fig. 3. Absorption spectra of the purified recombinant human kidney DAO, 16.4 mg mL^{-1} enzyme in 100 mM potassium phosphate buffer, pH 7.2

Fig. 4. Circular dichroism spectra of rhKDAO. Experimental conditions: 32 μM protein in 100 mM potassium phosphate buffer, pH 7.2, 1 nm resolution, 20 mdeg sensitivity, 1 s response, 500 μm slit, 5 accumulations
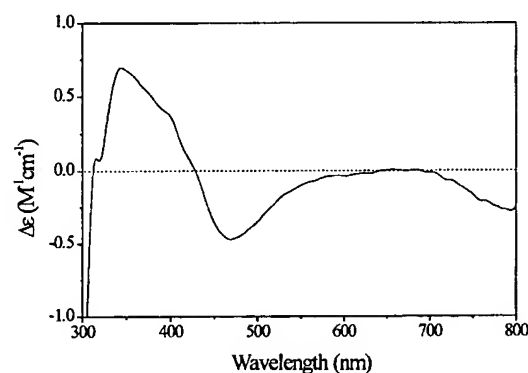
mol dimeric enzyme. In contrast, purified mammalian copper amine oxidases, as well as those from other organisms, are most often characterized as having two copper ions per dimer [1]. Our results indicate a correlation between copper content and specific activity for the recombinant enzyme; not surprisingly, samples with a higher copper content correspond to an increased specific activity.

Metal analysis and the lack of a manganese signal in the EPR spectra (Fig. 2) strongly suggest calcium occupies the putative second metal site in recombinant human kidney DAO. Purified enzyme was dialyzed either against metal-free 100 mM potassium phosphate buffer alone or against three changes of 2 L metal-free 100 mM potassium phosphate, 2 mM EDTA, pH 7.2, followed by extensive dialysis against metal-free phosphate buffer. The sample dialyzed against buffer alone was found by ICP emission spectroscopy to contain 2.37 mol calcium and 0.17 mol magnesium per mol of dimeric protein, whereas the sample treated with EDTA contained 2.16 mol calcium per homodimer, and magnesium levels were below the detection limit of the instrument.

Figure 2 shows the X-band EPR spectra of Cu(II) in purified rhKDAO. EPR parameters derived from simulated spectra ($g_\perp = 2.043$, $g_{||} = 2.265$, $A_{||} = 162$ G)

are consistent with published values for CAOs from various sources [1]. Crabbe et al. [34] reported a $g_\perp$ value of 2.05 from Q-band EPR spectra of purified human placental DAO; however, the presence of manganese prevented the determination of other copper parameters. Manganese was not removed by passing the protein over a Chelex 100 column, leading those investigators to conclude the human placental DAO was a Cu(II)-Mn(II) metalloprotein, with an apparent stoichiometry of 2.0 mol copper and 2.4 mol manganese per mol enzyme dimer. The lack of a characteristic six-line Mn(II) signal in our spectra is convincing evidence against any manganese associated with the recombinant enzyme.

The purified protein is peach colored with a broad visible absorption band having a λ_{max} at 470 nm (Fig. 3). This spectral feature is associated with the TPQ and gives copper amine oxidases their recognizable color. The shoulder in the absorption spectra at 400 nm is an unidentified feature, perhaps due to a modified (possibly incompletely processed) form of the cofactor. The CD spectrum shown in Fig. 4 exhibits a negative band around 470 nm that is attributed to TPQ and
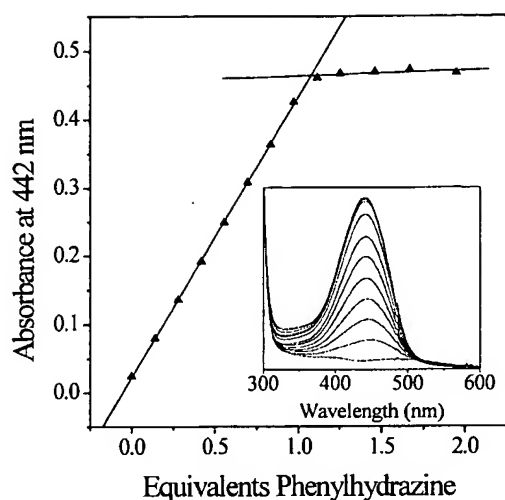
Fig. 5. Phenylhydrazine titration of TPQ in purified rhKDAO. Plot shows the change in absorbance at 442 nm versus equivalents phenylhydrazine added per enzyme dimer. One mL of enzyme (11.8 µM enzyme in 100 mM potassium phosphate buffer, pH 7.2) titrated with 2830 µM phenylhydrazine. The *inset* shows the increase in absoption of the intensely yellow-colored adduct with successive phenyhydrazine additions

a negative band around 800 nm from a Cu(II) d-d transition. These electronic transitions are consistent with other CAOs [1], and is consistent with a tetragonal Cu(II) complex with N,O donors.

Copper amine oxidases and the carbonyl reagent phenylhydrazine react to give a characteristic, yellow phenylhydrazone adduct that is commonly used to identify and quantify the TPQ cofactor [1]. Recombinant enzyme was titrated with phenylhydrazine and spectra were recorded after each addition when no further change in absorbance at 442 nm was noted. A typical titration demonstrating the formation of the intensely colored covalent adduct is shown in Fig. 5 and the results of TPQ quantification for three individual enzyme preparations are shown in Table 2. As described above for copper, the quantified organic cofactor correlates with specific activity.

The resonance Raman spectrum of phenylhydrazine-derivatized recombinant enzyme is shown in Fig. 6, along with that of the phenylhydrazone of TPQ-hydantoin, a model compound for the cofactor. Protein was concentrated after extensive buffer exchange to remove unreacted phenylhydrazine. The two spectra are essentially identical and thus conclusively identify TPQ as the quinone cofactor in the recombinant enzyme. Neither the visible absorption (Fig. 5) nor the resonance Raman spectrum of the phenylhydrazine adduct of rhKDAO suggests the absorption feature at ~400 nm (Fig. 3) reacts with this carbonyl reagent. Thus this unidentified absorption feature may be a modified form of the TPQ cofactor which is conformationally inaccessible to phenylhydrazine or one which is lacking a reactive carbonyl.
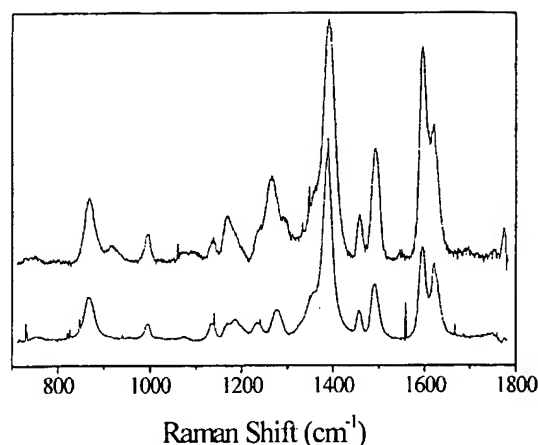

Fig. 6. Resonance Raman spectra of the phenyhydrazine-derivatized human rhKDAO (*upper spectrum*). The *lower spectrum* is the phenylhydrazine-derivatized model compound, TPQ-hydantoin. Experimental conditions: excitation 457.9 nm, power 40 mW, integration 1 min, 10 accumulations

Steady-state kinetics

K_M and k_{cat} were determined for several aliphatic diamines, the aromatic diamine DAB, and biologically important amines and polyamines. Initial rates were fit to the Michaelis-Menten equation and determined under the physiologically relevant conditions of 37 °C, pH 7.2, and an ionic strength of 150 mM. The results are summarized in Table 3.

Recombinant human DAO shows a substrate preference, as indicated by the specificity constant k_{cat}/K_M, for the diamines histamine (2-(4-imidazolyl)ethylamine) and 1-methylhistamine (1-methyl-4-[β-aminoethyl]imidazole), the metabolite of histamine N-methyltransferase (E.C.2.1.1.8). The aliphatic diamines putrescine and cadaverine give k_{cat}/K_M values close to, but lower than, those of the histidine metabolites. Histamine and 1-methylhistamine exhibit two of the three lowest turnover numbers, but note the turnover constants for all substrates investigated are quite similar and differ by less than a factor of 10. However, the determined K_M values vary by over three orders of magnitude, with the K_M for histamine about seven times less than that of any aliphatic diamine. The results of these experiments, namely that histamine and 1-methylhistamine are the preferred substrates, was completely unanticipated given the body of available literature, which inferred that the aliphatic diamines were the preferred substrates of human DAO (vide infra).

It should be kept in mind that the recombinant protein used for this work does not contain two copper ions and two organic cofactors per dimer; these experiments used rhKDAO with 1.42 copper ions and 1.04 titratable TPQ per dimer. Therefore the actual substrate turnover numbers for the natural hKDAO could be up to twice the values reported herein.

The pH dependence of k_{cat} for putrescine is shown in Fig. 7. The plot reveals a bell-shaped curve with
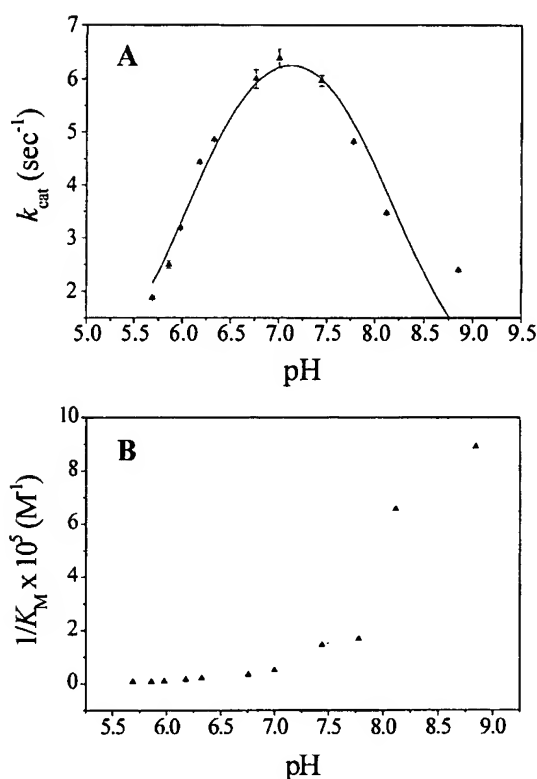
Table 3. Steady-state kinetic parameters and substrate specificity (k_{cat}/K_M) of rhKDAO. Errors are reported as standard error

Compound	K_M (µM)	k_{cat} (min^{-1})	k_{cat}/K_M (µM^{-1} min^{-1})
Histamine[c]	2.8 ± 0.07	139 ± 0.6	50 ± 1
1-Methylhistamine	3.4 ± 0.3	103 ± 1.5	30 ± 3
Putrescine[c]	20 ± 1	475 ± 11	24 ± 1
Cadaverine	30 ± 2	453 ± 14	15 ± 1
DAB	110 ± 4	548 ± 4.6	5.0 ± 0.2
1,3-Diaminopropane	130 ± 10	487 ± 23	3.8 ± 0.3
1,6-Diaminohexane	150 ± 20	293 ± 14	2.0 ± 0.3
Ethylenediamine	630 ± 10	126 ± 0.70	0.20 ± 0.003
Spermidine	1100 ± 480	187 ± 0.4	0.17 ± 0.07
L-Lysine methyl ester	2800 ± 110	345 ± 4.6	0.12 ± 0.005
(–)-Arterenol	$+$[a]	$+$	$+$
Benzylamine	$+$	$+$	$+$
3-Hydroxytyramine	$+$	$+$	$+$
Kynuramine	$+$	$+$	$+$
Spermine	$+$	$+$	$+$
5-Hydroxytryptamine	$-$[b]	$-$	$-$
L-Lysine	$-$	$-$	$-$
N^{α}-Acetyl-L-lysine methyl ester	$-$	$-$	$-$
Methylamine	$-$	$-$	$-$

[a]The positive symbol ($+$) denotes substrate oxidation could be detected, but at rates too low to determine kinetic parameters
[b]The negative symbol ($-$) indicates no rate was observed
[c]Partial substrate inhibition was observed only with histamine and putrescine

**Fig. 7A, B.** pH dependence of steady-state kinetic parameters for recombinant human kidney DAO. A k_{cat} versus pH. Fit to Eq. 4 gives two apparent pK_a values of 6.0 and 8.2. B $1/K_m$ versus pH

apparent pK_a values of 6.04 ± 0.06 and 8.22 ± 0.09. We attribute the lower pK_a to the ionization of the active site catalytic base *in the enzyme-substrate complex* (Asp373 in hKDAO). The higher pK_a likely represents the

ionization of the product Schiff base (Scheme 1, species B, C). Klinman and co-workers [36, 37] have described detailed work on the pH dependence of steady-state parameters for the CAOs from bovine plasma and a yeast, and our data are consistent with their interpretation. A plot of $1/K_M$ versus pH reflects ionization potentials in the free enzyme and free substrate [29]. As shown in Fig. 7, the reciprocal Michaelis constant for rhKDAO is relatively constant from pH 5.7 to pH 7.0 and increases at higher pH values. These data could not be used to determine apparent pK_a values, although the data are in agreement with the interpretation of Klinman and co-workers of the catalytic aspartate residue in the free enzyme (Scheme 1, A) having an unusually high apparent pK_a (~8) and dramatically decreasing by about two orders of magnitude upon substrate binding.

Partial substrate inhibition was observed with histamine and putrescine (Fig. 8). Bardsley et al. [38] have previously described substrate inhibition with pig kidney DAO and attributed this inhibition as a primary kinetic salt effect, suggesting enzyme and substrate association might be partially rate limiting. Data for histamine and putrescine were fit to Eq. 3, which describes classical substrate inhibition where a second molecule of substrate binds to the enzyme-substrate complex to give a catalytically inactive complex. Panel B demonstrates that, at histamine concentrations of up to 250 µM, rhKDAO closely fits this model of substrate inhibition. However, at higher substrate concentrations (panel C) the data deviate from this model, suggesting that at higher histamine concentrations the enzyme kinetics are more complicated than the classical description of substrate inhibition. Figure 8C also shows the striking difference in kinetic behavior between histamine and 1-methylhistamine. Methylation of the imadazole
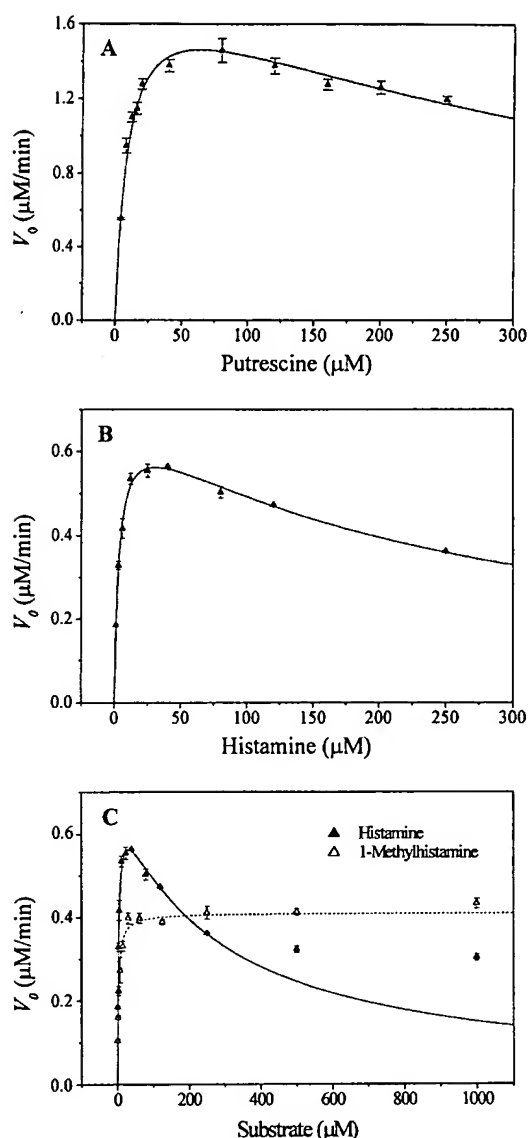
Fig. 8A–C. Plots of initial rates of reaction versus substrate concentration, demonstrating substrate inhibition observed with rhKDAO. Putrescine and histamine data were fit to Eq. 3; 1-methylhistamine data were fit to the Michaelis-Menten equation. A Putrescine substrate, $K_i = 430 \pm 40$ µM (0.8 µg enzyme at 1.00 IU mg^{-1} in a 1 mL assay volume, 50 mM HEPES, pH 7.5, ionic strength adjusted to 150 mM with KCl, at 37 °C). **B** Histamine substrate, $K_i = 280 \pm 30$ µM. **C** Comparison of histamine and 1-methylhistamine. Histamine and 1-*N*-methylhistamine assays used 7.3 µg enzyme (1.17 IU mg^{-1}) in a 1 mL assay volume, 50 mM HEPES, pH 7.2, ionic strength adjusted to 150 mM with KCl, at 37 °C

nitrogen apparently abolishes the substrate inhibition observed with histamine.

Two recent reports have suggested porcine kidney DAO is inhibited by heparin, either during prolonged binding on a heparin affinity column or through exposing the enzyme to free heparin [39, 40]. To investigate the possible effects of heparin on rhKDAO and to determine whether or not this is a general phenomenon of mammalian DAOs, the purified recombinant enzyme

was incubated with an approximately two-fold excess of heparin over heparin-binding sites. K_M and k_{cat} values were not noticeably different from untreated protein for up to 72 h. Additionally, no correlation between specific activity and length of time the protein was bound to the heparin affinity column during purification was discerned.

Tissue-specific expression

A commercially available array of polyA$^+$ RNA representing 76 different human tissues and cell lines was probed with ^{35}P-labeled kidney DAO cDNA probes. The amount of polyA$^+$ RNA dotted on the nylon membrane was normalized by the manufacturer to give similar signal intensities for eight housekeeping genes and therefore varies from 53 to 780 ng. Each dot is 1 mm in diameter. Exposed and developed X-ray film is shown in Fig. 9. Although the data are not quantifiable, a qualitative interpretation is informative for comparative analysis of tissue-specific gene expression. The highest levels of DAO gene expression are in the placenta, followed by kidney tissue. Exposure at these two mRNA spots has clearly over-saturated the photographic media. Therefore actual mRNA levels may be orders of magnitude greater than that indicated by examination of the film. Gene expression is detectable in stomach tissue and quite significant through the distal tissues of the gastrointestinal tract. Prostate and liver tissues also show fairly strong signals. A positive can be seen with *E. coli* DNA; however, kidney DAO cDNA and the bacterial genome have no significant sequence homology, and this is assumed to be a false positive. A similar false positive has previously been reported [41]. Low, but detectable, positive results are seen in tissues from the stomach, bone marrow, lung, pancreas, testis, lymph node, and the parietal lobe and pons of the human brain. Negative results for controls other than the *E. coli* DNA, as well as for the majority of human tissues and cell lines, suggest that these are genuine positives. However, the weak results for these tissues, as compared to strong signals from other tissues, are such that actual gene expression levels in these tissues are normally quite low.

Discussion

Human kidney DAO, under the control of the metallothionein promoter, has been expressed in a *Drosophila* S2 polyclonal cell line. This work describes the first overexpression and purification of a copper-containing amine oxidase from any animal source. Expression levels for the secreted, recombinant enzyme are substantial, approaching 20 mg L^{-1} of cell culture. Almost certainly the abundant rhKDAO is a consequence of stably transfected *Drosophila* S2 cell lines generally containing multicopy genomic inserts of the

Fig. 9. Multiple human tissue expression array with polyA mRNA from 76 tissues and cell lines (Clontech). Probed with randomly primed ^{32}P-labeled oligonucleotides generated by PCR from a cDNA clone of human kidney DAO

	1	2	3	4	5	6	7	8	9	10	11	12
A	whole brain	cerebellum, left	substantia nigra	heart	esophagus	colon, transverse	kidney	lung	liver	leukemia, HL-60	fetal brain	yeast total RNA
B	cerebral cortex	cerebellum, right	accumbens nucleus	aorta	stomach	colon, descending	skeletal muscle	placenta	pancreas	HeLa S3	fetal heart	yeast tRNA
C	frontal lobe	corpus callosum	thalamus	atrium, left	duodenum	rectum	spleen	bladder	adrenal gland	leukemia, K-562	fetal kidney	E. coli rRNA
D	parietal lobe	amygdala	pituitary gland	atrium, right	jejunum		thymus	uterus	thyroid gland	leukemia, MOLT-4	fetal liver	E. coli DNA
E	occipital lobe	caudate nucleus	spinal cord	ventricle, left	ileum		peripheral blood leukocyte	prostate	salivary gland	Burkitt's lymphoma, Raji	fetal spleen	Poly r(A)
F	temporal lobe	hippo-campus		ventricle, right	ileocecum		lymph node	testis	mammary gland	Burkitt's lymphoma, Daudi	fetal thymus	human C$_t$-1 DNA
G	p.g.* of cerebral cortex	medulla oblongata		inter-ventricular septum	appendix		bone marrow	ovary		colorectal adeno-carcinoma SW480	fetal lung	human DNA 100 ng
H	pons	putamen		apex of the heart	colon, ascending		trachea			lung carcinoma A549		human DNA 500 ng

* paracentral gyrus

expression and selection plasmids, often with 500–1000 copies arranged in a head-to-tail fashion [42]. Very recently, Koyanagi and co-workers [43] reported the heterologous overexpression of a copper amine oxidase from a multicellular organism, the plant *P. sativum*. Unfortunately, low expression levels and considerable clonal variation mar this notable accomplishment (Tanizawa K, personal communication). Expression of the *Arabidopsis thaliana* enzyme has previously been described in a baculovirus expression system [44]. The natural hKDAO heparin-binding site facilitated the development of a rapid purification scheme, resulting in the highly efficient recovery of >98% homogeneous protein. We present herein the first detailed spectroscopic investigation and characterization of a highly purified, recombinant human copper-containing amine oxidase.

Expression in serum-free media avoids introduction of exogenous copper amine oxidases [45, 46], as well as the considerable amount of undesired proteins naturally present in fetal calf serum. Furthermore, searches

of the *D. melanogaster* genome have not revealed any sequences with significant homology to CAOs, nor, to the best of our knowledge, has a CAO been described from any insect source. However, one member of the copper-containing amine oxidase family, lysyl oxidase (E.C. 1.4.3.13), has been identified in the *Drosophila* genome [47]. Lysyl oxidase contains a lysine-tyrosyl-quinone cofactor and catalyzes the oxidative deamination of peptidyl lysine in elastin and collagen – a crucial step for connective tissue cross-linking [48]. Therefore the *Drosophila* Expression System, when used with serum-free media, is an excellent source of secreted human DAO, with the inherent advantages of low levels of unwanted proteins and apparently no contaminating CAOs, either exogenous or endogenous. *Drosophila* S2 cell have previously been used to express another copper enzyme, human dopamine β-hydroxylase, at protein yields quite similar to those reported in this work [49]. This expression system is thus a promising option for the convenient expression of other eukaryotic metalloenzymes.

Analytical ultracentrifugation results suggest rhKDAO contains between 20 and 26% glycosylation by weight, a value not unreasonable for the natural mammalian enzyme. The results given by Crabbe et al. [34] indicate approximately 40% glycosylation for the natural human placental enzyme. Gel filtration by Baylin and Margolis [35] suggest 20% glycosylation for the natural human pregnancy plasma DAO. For comparison, the porcine kidney DAO has been estimated at 20% and 11% carbohydrate by weight [50, 51]. Although the data on glycosylation in mammalian DAOs are limited – and it must be noted that differences in glycosylation could very well be tissue-specific – the extent of glycosylation by weight in rhKDAO is within the range of values reported for the natural enzymes.

SDS/PAGE and analytical ultracentrifugation results are consistent with a substantially glycosylated recombinant enzyme, as would be expected for a protein with potential glycosylation sites and processed through the secretory pathway. Electrospray mass spectrometry of the recombinant human kidney protein gave a large m/z "hump" with no resolvable peaks, indicative of a population of heterogeneously glycosylated proteins (data not shown). Four consensus N-glycosylation sequences (NXS/T) are present in the peptide sequence of human kidney DAO. N-Linked glycosylation in *Drosophila* is much like that in other insect cells, with a high mannose content, although O-linked glycosylation is also possible [52, 53]. Glycosylation of the recombinant enzyme is expected to be different from the enzymes processed in mammalian cells, and strategies to reduce the extent of glycosylation in rhKDAO are actively being pursued.

The heterologously expressed enzyme contains substoichiometric copper and displays some variability in copper levels from different purifications. The data shown in Table 2 indicate the copper content ranges from 1 to 1.5 ions per dimer. The recombinant enzyme most likely contains tightly bound zinc in the remaining active sites; copper and zinc together account for nearly full metal occupancy of the two active sites in each protein homodimer. Zinc has previously been described in recombinant *H. polymorpha* CAO overexpressed in *Saccharomyces cerevisiae*, and zinc was determined to have a high affinity for the active site and to compete with copper for binding [54]. The crystal structure of a zinc-substituted *H. polymorpha* enzyme has recently been solved and reveals zinc in the active site, coordinated by three histidine residues and a tyrosine residue (copper ligands in the active enzyme and the tyrosine precursor of TPQ) [55]. These residues are remarkably similar in position to those described in the active site of apoCAO from *Arthrobacter globiformis* [15].

We believe active-site metal incorporation most likely occurs intracellularly during rhKDAO processing in the *Drosophila* secretory pathway, and not following secretion into media loaded with 500 μM copper, in which case fully copper-loaded protein could be expected. Rae et al. [56] have made a convincing argument for extraordinarily low levels of "free" intracellular copper, less than one per cell, and suggested copper-dependent enzymes require accessory factors (i.e. metallochaperones). However, their analysis is based upon *cytoplasmic* superoxide dismutase and would not necessarily apply to the contents of membrane-bound organelles, such as those of the secretory pathway. Copper most likely enters the *Drosophila* secretory pathway via a P-type ATPase, homologous to the human Menkes disease protein, localized in the trans-Golgi network [57]. To date, no accessory protein for any CAO has been described. Furthermore, *Drosophila* S2 culture is quite likely a zero background expression host and therefore would not be expected to possess a specific CAO metallochaperone. Copper and zinc content in the overexpressed enzyme may be determined by the total metal ion availability in the secretory pathway and the relative affinity of the active site for these two transition metals. Differences in metal loading between purifications might be the consequence of subtle and as yet unrecognized factors during cell culturing and protein expression.

This study indicates calcium occupies the putative second metal binding site in recombinant human kidney DAO. The high specificity and affinity of this site for calcium, supported by the resistance to removal by EDTA ($\log K = 10.61$ at 25 °C [58]), strongly suggest calcium would be present in the natural enzyme. Stoichiometric calcium is also present in highly purified equine plasma copper amine oxidase (unpublished results).

Although calcium sites in proteins vary considerably with regard to their coordination structure, the second-metal site in copper amine oxidases is unusual when compared to other structurally defined sites (see [59] for a recent review of the diverse calcium binding sites in proteins). Five putative KDAO calcium ligands can be deduced from sequence alignment and the crystal structures of the CAOs from *E. coli* and *P. sativum* [13, 14]. Three of these are aspartyl carboxylates and the backbone carbonyl of a leucine in the sequence AspLeuAsp. These residues are located at the C-terminus of one β strand. The other two protein-derived oxygen donors are an aspartyl carboxylate and an adjacent backbone carbonyl (Leu), located at the N-terminus of another β strand. Interestingly, the opposite ends of these two β strands (7–10 residues away) also provide the active site copper ligands. One coordinating water molecule is resolved in the crystal structures, giving an octahedral coordination geometry with calcium-oxygen distances from 2.2 to 2.5 Å. Most calcium ions in biology are heptacoordinate and associated with helical and loop regions [60]. The well-known and extensive family of helix-loop-helix (EF hand) calcium sites is typically seven-coordinate with three carboxylates (one of which is bidentate), two carbonyls, and one water molecule in a pentagonal bipyramid. EF hand ligands are all located in a short sequence at the end of one helix, a small loop, and the beginning of another helix. In contrast, the calcium binding residues in CAOs are at the ends of two

β strands, separated in sequence by more than 130 intervening amino acids.

Calcium ions are critical for a variety of important biological processes, including some involving extracellular proteins [61, 62, 63, 64, 65, 66]. The function of the second metal site in copper-containing amine oxidases remains to be elucidated. However, the bound calcium ion likely serves to stabilize the structure of this extracellular enzyme, although a role in modulating activity is also possible but unlikely, given the apparently high affinity for calcium and the separation between the putative Ca site and the active site.

Recombinant human kidney DAO is conclusively demonstrated to possess the TPQ cofactor. Visible absorption, CD, titration with phenylhydrazine, and resonance Raman of the phenylhydrazine-derivatized enzyme are entirely consistent with previously characterized copper amine oxidases from various sources [1, 67]. Similar correlations between specific activity and titratable TPQ have been described by Klinman and co-workers [23, 68] for the bovine plasma amine oxidase and the recombinant yeast methylamine oxidase. As shown in Table 2, the titratable TPQ from three different preparations is consistently around 72% of that which could be expected given the copper to protein stoichiometry, assuming that each active site containing copper would readily convert the precursor tyrosine to TPQ. It is presently unclear whether low TPQ-to-copper ratios reflect incomplete organic cofactor biogenesis or enzyme conformations in which the quinone cofactor is inaccessible to phenylhydrazine. Low and variable TPQ content is not uncommon in CAOs [1]. For example, recombinant yeast methylamine oxidase has been described as containing 2.0 mol copper but only 1.5 mol phenylhydrazine-titratable TPQ per mol of enzyme dimer [68], a TPQ to copper ratio strikingly close to the results presented herein.

Recombinant human kidney DAO shows a clear substrate preference for diamines, with the highest specificity constants (k_{cat}/K_M) for histamine and 1-methylhistamine. It is also apparent that substrate specificity depends on the separation between the substrate's two amine groups, as well as other structural features. Although diaminopropane is a good substrate, the polyamine spermine, also with three methylene carbons between a primary amine nitrogen and the closest secondary amine, is a very poor substrate, with an oxidation rate nearly undetectable using our assay conditions. Spermidine, on the other hand, has four methylene carbons between one of the primary amines and the secondary amine and is a fair substrate, but with a specificity constant two orders of magnitude less than that for putrescine. L-Lysine methyl ester is a poor substrate, and no oxidation was observed with either L-lysine or N^α-acetyl-L-lysine methyl ester. Therefore, it is extremely unlikely that the DAO-catalyzed oxidation of peptidyl lysines would occur to a physiologically relevant extent in vivo.

Earlier literature reported the substrate preference of DAO solely determined by relative rates of oxidation, a necessary criterion given the limited amounts of enzyme available. Misleading conclusions regarding substrate preference were inevitable, given the difficulty in obtaining highly purified mammalian DAO, partial substrate inhibition, and the millimolar substrate concentrations used. Generally, cadaverine was reported as the substrate with highest rate of oxidation, up to nearly 1.5 times the rate for putrescine. Histamine was described as having only 17–50% the relative rate of oxidation as compared to putrescine [32, 34, 69]. Unfortunately, this has resulted in a predisposition to downplay or discount a possible role for DAO in histamine metabolism in much of the earlier literature.

Our work establishes a K_M for histamine equal to 2.8 µM and a k_{cat}/K_M of 50 µM^{-1}min^{-1}. Previously reported K_M values for DAO purified from human tissues range from 1.5 µM for the enzyme isolated from pregnancy serum to 19 µM for the intestinal DAO [30, 70, 71]. The apparent K_M determined for 1-methylhistamine is 3.4 µM, whereas earlier work reported 97 µM [30, 71]. It is interesting to note that aliphatic diamines and polyamines would be protonated at physiological pH and therefore be di- or polycationic. Histamine, however, would only be about 8% present as the doubly charged species at pH 7.2.

The recombinant enzyme exhibits an apparent K_M for putrescine of 20 µM. Previously reported values from purified human DAOs range from 13 µM to 83 µM [30, 71, 72]. Höltta et al. [72] reported that human seminal plasma DAO displays a K_M of 100 µM for spermine and 560 µM for spermidine. In contrast, we find an apparent K_M of 1.1 mM for spermidine, and that of spermine could not be determined with our experimental conditions. This discrepancy is perhaps due to contaminating enzymes in the seminal plasma enzyme purification or impurities in commercially available polyamines; in fact, Höltta and co-workers described contaminating spermidine and putrescine in purchased spermine.

Scheme 1 diagrams the proposed steps in the catalytic cycle of CAOs [73, 74]. Detailed kinetic studies have elucidated many of the details of the reductive half-reaction. Proton abstraction from the substrate Schiff base (species B) has been shown to at least partially contribute to the rate-determining step in some mammalian CAOs [36, 75]. Substrate turnover (k_{cat}) values for rhKDAO are quite similar among the substrates investigated in this work, from 1 to 10 s^{-1}, suggesting a common rate-limiting step.

The oxidative-half reaction is less well understood. Anaerobic substrate-reduced enzyme has been shown to be a kinetically competent, equilibrium mixture of the Cu(II)-aminoquinol and Cu(I)-aminosemiquinone radical (species D, E), and substantial chemical precedence suggests the Cu(I)-aminosemiquinone species would readily react with dioxygen [76, 77, 78]. However, an obligatory role for Cu(I) has not been established, and a

viable mechanistic alternative that does not invoke a change in the oxidation state of copper has been proposed [79, 80]. Copper amine oxidases from different sources have been suggested to use distinctly different mechanisms for reoxidation [81]. We anticipate that the work presented herein will facilitate experimental design to probe the molecular details of TPQ reoxidation and the concomitant reduction of dioxygen in the human enzyme.

Biological implications

Mammalian DAOs are found in several tissues, with the highest activities described in placenta, small intestine, and kidney, but they are also present in liver, lung, fibroblasts, salivary glands, and seminal fluid. Low basal levels of DAO are present in human serum and are believed to derive from the gastrointestinal tract [1]. However, the circulatory DAO activity increases significantly following the intravenous injection of heparin and during pregnancy [82, 83, 84, 85, 86].

The human expression array results presented herein largely concurs with earlier studies describing the tissues with highest DAO activity, but some of the positive results were unanticipated. To the best of our knowledge, DAO activity has not been reported in lymph nodes or bone marrow, and the expression array indicates positive, albeit low, DAO mRNA in two specific regions of the human brain, the parietal lobe and the pons. It will be of considerable interest to see if future studies support the apparent localized expression of DAO in the human brain. DAO activity in this organ is normally extremely low [87, 88]. However, evidence exists for increased DAO activity in rat brain following focal brain injury, an increase that tracks the rise in putrescine concentration [89]. DAO is generally not thought to play a role in histamine metabolism in the brain, where histamine serves as a neurotransmitter. The physiological function (or functions) of this enzyme in the human brain remains to be demonstrated.

Several investigations have reported putrescine (1,4-diaminobutane) or cadaverine (1,5-diaminopentane) as the substrate with the highest rate of oxidation and suggested these are the preferred substrates for mammalian DAOs [30, 32, 34, 72, 90, 91]. Putrescine deamination is the rate-limiting step in catabolism of the polyamines spermidine and spermine [92]. These polyamines are found in millimolar concentrations in cells and in seminal fluid and are important in cell proliferation and differentiation [1, 93, 94]. Given the steady-state parameters determined in this work, putrescine and spermidine could be viable substrates for the DAO known to be present extracellularly (e.g., recall that the expression array gives a strong positive for the prostrate). Additionally, γ-aminobutyraldehyde, the product of putrescine oxidation by DAO, is a precursor for the neurotransmitter γ-aminobutyric acid in some tissues [95].

The current work, however, indicates a substrate preference for histamine and 1-methylhistamine, suggesting human DAO may play an important role in histamine metabolism. Histamine is a potent pharmacological agent with profound biological effects, including smooth muscle contraction, vasodilation, allergic response, gastric acid secretion, and stimulation of adenylate cyclase activity in neurons, all of which are mediated by specific G-protein-coupled receptors [96].

Historically, DAO has been proposed to function as a safeguard against deleterious effects from exogenous amines. In the intestinal tract this enzyme is thought to detoxify ingested histamine [30, 97] and in placental tissues is suggested to protect from high levels of fetal putrescine and histamine [98, 99]. However, the striking substrate inhibition observed with histamine seems to make DAO an unlikely choice to serve as the first line of defense against toxic levels of histamine. In circulation, histamine concentrations are usually only a few micromolar, a physiologically relevant condition in which DAO could be very efficient in removing undesired histamine. Baenziger, Haddock and co-workers [45] have demonstrated DAO activity enhances histamine metabolism and uptake by cultured vascular endothelial cells and have proposed that DAO in circulation can bind to specific endothelial cell surface receptors and participate in the sequential, enzymatic degradation of histamine. Collectively, the available evidence suggests that DAO may be involved in several critical biological processes in mammals, perhaps depending in part on spatial and temporal factors, as well as the level of expression.

References

1. McIntire WS, Hartmann C (1993) In: Davidson VL (ed) Principles and applications of quinoproteins. Dekker, New York, pp 97–171
2. Janes SM, Palcic MM, Scaman CH, Smith AJ, Brown DE, Dooley DM, Mure M, Klinman JP (1992) Biochemistry 31:12147–12154
3. Matsuzaki R, Fukui T, Sato H, Ozaki Y, Tanizawa K (1994) FEBS Lett 351:360–364
4. Cai D, Klinman JP (1994) J Biol Chem 269:32039–32042
5. Ruggiero CE, Smith JA, Tanizawa K, Dooley DM (1997) Biochemistry 36:1953–1959
6. Dooley DM (1999) J Biol Inorg Chem 4:1–11
7. Morris NJ, Ducret A, Aebersold R, Ross SA, Keller SR, Lienhard GE (1997) J Biol Chem 272:9388–9392
8. Mu D, Medzihradszky KF, Adams GW, Mayer P, Hines WM, Burlingame AL, Smith AJ, Cai D, Klinman JP (1994) J Biol Chem 269:9926–9932
9. Zhang XP, McIntire WS (1996) Gene 179:279–286
10. Salminen TA, Smith DJ, Jalkanen S, Johnson MS (1998) Protein Eng 11:1195–1204
11. Moldes M, Feve B, Pairault J (1999) J Biol Chem 274:9515–9523
12. Novotny WF, Chassande O, Baker M, Lazdunski M, Barbry P (1994) J Biol Chem 269:9921–9925

13. Parsons MR, Convery MA, Wilmot CM, Yadav KDS, Blakeley V, Corner AS, Phillips SEV, McPherson MJ, Knowles PF (1995) Structure 3:1171–1184
14. Kumar V, Dooley DM, Freeman HC, Guss JM, Harvey I, McGuirl MA, Wilce MCJ, Zubak VM (1996) Structure 4:943–955
15. Wilce MCJ, Dooley DM, Freeman HC, Guss JM, Matsunami H, McIntire WS, Ruggiero CE, Tanizawa K, Yamaguchi H (1997) Biochemistry 36:16116–16133
16. Li RB, Klinman JP, Mathews FS (1998) Structure 6:293–307
17. Scott RA, Dooley DM (1985) J Am Chem Soc 107:4348–4350
18. Dooley DM, McGuirl MA, Cote CE, Knowles PF, Singh I, Spiller M, Brown RD III, Koenig SH (1991) J Am Chem Soc 113:754–761
19. McCracken J, Peisach J, Dooley DM (1987) J Am Chem Soc 109:4064–4072
20. Gill SC, Von Hippel PH (1989) Anal Biochem 182:319–326
21. Holmquist B, Vallee BL (1973) Biochemistry 12:4409–4417
22. Szutowicz A, Kobes RD, Orsulak PJ (1984) Anal Biochem 138:86–94
23. Janes SM, Klinman JP (1991) Biochemistry 30:4599–4605
24. Orville AM, Lipscomb JD (1997) Biochemistry 36:14044–14055
25. Bardsley WG, Crabbe MJC, Shindler JS, Ashford JS (1972) Biochem J 127:875–879
26. Holt A, Sharman DF, Baker GB, Palcic MM (1997) Anal Biochem 244:384–392
27. Ruggiero CE, Dooley DM (1999) Biochemistry 38:2892–2898
28. Cleland WW (1979) Methods Enzymol 63:500–513
29. Fersht A (1999) Structure and mechanism in protein science. Freeman, New York
30. Bieganski T, Kusche J, Lorenz W, Hesterberg R, Stahlknecht C-D, Feussner K-D (1983) Biochim Biophys Acta 756:196–203
31. Bjellqvist B, Hughes GJ, Pasquali C, Paquet N, Ravier F, Sanchez JC, Frutiger S, Hochstrasser D (1993) Electrophoresis 10:1023–1031
32. Suzuki O, Matsumoto T (1987) Biogenic Amines 4:237–245
33. Bardsley WG, Crabbe MJ, Scott IV (1974) Biochem J 139:169–181
34. Crabbe MJC, Waight RD, Bardsley WG, Barker RW, Kelly I, Knowles PF (1976) Biochem J 155:679–687
35. Baylin SB, Margolis S (1975) Biochim Biophys Acta 397:294–306
36. Farnum M, Palcic M, Klinman JP (1986) Biochemistry 25:1898–1904
37. Hevel JM, Mills SA, Klinman JP (1999) Biochemistry 38:3683–3693
38. Bardsley WG, Crabbe MJC, Shindler JS (1973) Biochem J 131:459–469
39. Wilflingseder D, Schwelberger HG (2000) J Chromatogr B Biomed Sci Appl 737:161–166
40. Wilflingseder D, Klocker J, Schwelberger HG (2000) Inflamm Res 49:S55–S56
41. Jakobbson P-J, Thoren S, Morgenstern R, Samuelsson B (1999) Proc Natl Acad Sci USA 96:7220–7225
42. Invitrogen (1998) Drosophila expression system, version C. Invitrogen, Carlsbad, Calif
43. Koyanagi T, Matsumura K, Kuroda S, Tanizawa K (2000) Biosci Biotech Biochem 64:717–722
44. Moller SG, McPherson MJ (1998) Plant J 13:781–791
45. Haddock RC, Mack P, Fogerty FJ, Baenziger NL (1987) J Biol Chem 262:10220–10228
46. Gahl WA, Pitot HC (1982) Biochem J 202:603–611
47. FlyBase (1999) Nucleic Acids Res 27:85–88
48. Wang SX, Mure M, Medzihradszky KF, Burlingame AL, Brown DE, Dooley DM, Smith AJ, Kagan HM, Klinman JP (1996) Science 273:1078–1084
49. Li B, Tsing S, Kosaka AH, Nguyen B, Osen EG, Bach C, Chan H, Barnett J (1996) Biochem: J 313:57–64
50. Rinaldi A, Vecchini P, Floris G (1982) Prep Biochem 12:11–28
51. Schwelberger HG, Bodner E (1997) Biochim Biophys Acta 1340:152–164
52. Jarvis DL, Finn EE (1995) Virology 212:500–511
53. Culp JS, Johansen H, Hellmig B, Beck J, Matthews TJ, Delers A, Rosenberg M (1991) Biotechnology (NY) 9:173–177
54. Cai DY, Williams NK, Klinman JP (1997) J Biol Chem 272:19277–19281
55. Chen ZW, Schwartz B, Williams NK, Li RB, Klinman JP, Mathews FS (2000) Biochemistry 39:9709–9717
56. Rae TD, Schmidt PJ, Pufahl RA, Culotta VC, O'Halloran TV (1999) Science 284:805–808
57. Yamaguchi Y, Heiny ME, Suzuki M, Gitlin JD (1996) Proc Natl Acad Sci USA 93:14030–14035
58. Martell AE, Smith RM (1974) Critical stability constants, vol 1: amino acids. Plenum Press, New York
59. Pidcock E, Moore GR (2001) J Biol Inorg Chem 6:479–489
60. McPhalen CA, Strynadka NCJ, James MNG (1991) In: Anfinsen CB, Edsall JT, Richards FM, Eisenberg DS (eds) Advances in protein chemistry, vol 42. Academic Press, San Diego, pp 77–144
61. Sutherland GR, Aust SD (1996) Arch Biochem Biophys 332:128–134
62. Feder J, Garrett LR, Wildi BS (1971) Biochemistry 10:4552–4556
63. Drucker H, Borchers SL (1971) Arch Biochem Biophys 147:242–248
64. McDonald MR, Kunitz M (1941) J Gen Physiol 25:53–73
65. Sipos T, Merkel JR (1970) Biochemistry 9:2766–2775
66. Dennis EA (1994) J Biol Chem 269:13057–13060
67. Brown DE, McGuirl MA, Dooley DM, Janes SM, Mu D, Klinman JP (1991) J Biol Chem 266:4049–4051
68. Cai D, Klinman JP (1994) Biochemistry 33:7647–7653
69. Holtta E, Pulkkinen P, Elfving K, Janne J (1975) Biochem J 145:373–378
70. Zeiger RS, Yurdin DL, Colten HR (1976) J Allergy Clin Immunol 58:172–179
71. Bieganski T, Kusche J, Feussner KD, Hesterberg R, Richter H, Lorenz W (1980) Arch Immunol Ther Exp 28:901–906
72. Höltta E, Pulkkinen P, Elfving K, Janne J (1975) Biochem J 145:373–378
73. Knowles PF, Dooley DM (1994) In: Sigel H, Sigel A (eds) Metal ions in biological systems, vol 30. Dekker, New York, pp 361–403
74. Klinman JP (1996) Chem Rev 96:2541–2561
75. Bardsley WG, Crabbe MJC, Scott IV (1974) Biochem J 139:169–181
76. Dooley DM, McGuirl MA, Brown DE, Turowski PN, McIntire WS, Knowles PF (1991) Nature 349:262–264
77. Turowski PN, McGuirl MA, Dooley DM (1993) J Biol Chem 268:17680–17682
78. Dooley DM, Brown DE (1996) J Biol Inorg Chem 1:205–209
79. Su QJ, Klinman JP (1998) Biochemistry 37:12513–12525
80. Mills SA, Klinman JP (2000) J Am Chem Soc 122:9897–9904
81. Padiglia A, Medda R, Bellelli A, Agostinelli E, Morpurgo L, Mondovi B, Finazzi-Agrò A, Floris G (2001) Eur J Inorg Chem 1:35–42
82. Hansson R, Holmberg CG, Tibbling G, Tryding N, Westling H, Wetterqvist H (1966) Acta Med Scand 180:533–536
83. Weingold AB (1968) Clin Obstet Gynecol 11:1081–1105
84. Hansson R, Thysell H (1971) Acta Physiol Scand 81:208–214
85. Klocker J, Drasche A, Sattler J, Bodner E, Schwelberger HG (2000) Inflamm Res 49:S53–S54
86. Rokkas T, Vaja S, Taylor P, Murphy GM, Dowling RH (1990) Digestion 46-S2:439–446
87. Seiler N, Al-Therib, MJ (1974) Biochem J 144:29–35
88. Brown RE, Stevens DR, Haas HL (2001) Prog Neurobiol 63:637–672
89. Desiderio MA, Zini I, Davalli P, Zoli M, Corti A, Fuxe K, Agnati LF (1988) J Neurochem 51:25–31
90. Bardsley WG, Hill CM, Lobley RW (1970) Biochem J 117:169–176
91. Bieganski T, Kusche J, Feussner KD, Hesterberg R (1980) Agents Actions 10:108–110
92. Sessa A, Perin A (1994) Agents Actions 43:69–77

93. Watanabe S, Kusama-Eguchi K, Kobayashi H, Igarashi K (1991) J Biol Chem 266:20803–20809
94. Sussman JL, Harel M, Frolow F, Oefner C, Goldman A, Toker L, Silman I (1991) Science 253:872–879
95. Seiler N (1980) Physiol Chem Phys 12:411–429
96. Rangachari PK (1992) Am J Physiol 262:G1–G13
97. Baylin SB, Beaven MA, Buja LM, Keiser HR (1972) Am J Med 53:723–733
98. Kapeller-Adler R (1970) Amine oxidases and methods for their study. Wiley, New York
99. Bardsley WG, Crabbe MJC (1973) Biochem Soc Trans 1:494–496